Est. 1984

**ORIENTAL JOURNAL OF CHEMISTRY**
An International Open Access, Peer Reviewed Research Journal

www.orientjchem.org

ISSN: 0970-020 X
CODEN: OJCHEG
2023, Vol. 39, No.(3):
Pg. 627-634

# A Novel Study on 2-D Material in Photoelectrochemical Cell for the Conversion and Storage of Solar Energy

**SHANKER LAL MEENA[1], KAVITA MEENA[2]*, RAVI KUMAR BHUPESH[3] and R. C. MEENA[4]**

[1,2,3,4]Photoelectrochemical Laboratory, Department of Chemistry,
Jai Narain Vyas University, Jodhpur, 342001, India.
*Corresponding author E-mail: slmeena.jnvu@gmail.com

http://dx.doi.org/10.13005/ojc/390313

(Received: April 01, 2023; Accepted: May 04, 2023)

**ABSTRACT**

A photo-sensitizer made of graphene-based material (2-D) is used in concert with EDTA in photoelectrochemical solar cells to increase efficiency and storage capacity of solar energy in order to make a solar cell economically feasible. Photopotential and photocurrent are created at 1142mV and 960 µA, respectively. Photoelectrochemical cell have achieved a maximum power of 228.40 µW, a fill factor of 0.17, and a conversion efficiency of 4.38%. The cell storage capacity allows for a half power ($t_{1/2}$) level to be maintained for 1300 minutes. The electrical output of the photoelectrochemical cell has been observed to be influenced by a number of different factors.

**Keywords:** 2-D materials, Photoelectrochemical cell, Photo potential, Photocurrent, Conversion efficiency.

## INTRODUCTION

In future, there will be a huge global demand for energy. The energy production from the traditional methods arise pollution in the environment. Therefore, the field of renewable energy storage and focus field of the research.[1] hence, the need of such devices for the effective use of renewable energy and such type of devices should be maximum efficient, cheaper-price and eco-friendly.[2] Photoelectrochemical solar cells are the good devices for the production of high energy chemicals from the sun light. Due to their abundance, stability and eco-friendliness is most suitable and intense field of the research.[3]

In recent years, scientific community has founded that the study of carbon allotropes (carbon nanotube, diamond and fullerene) is more emerged area of research.[4] Graphene is a two-dimensional (2D) carbon atom that was discovered in the year 2004.[5] It is a monolayer and crystal honeycomb lattice structure. Konstantin Novoselov and Andre Geim awarded the 2010 Nobel Prize in Physics based on their research on two-dimensional graphene.It is called the mother of all graphite forms of carbon. To produce low-cost, lightweight, and high-performance composite materials, researchers from all over the world are still exploring for new dimensions. The basic building block for other allotropes is thought to be graphene.[6] Carbon atoms

are arranged in a two-dimensional honeycomb lattice called graphene, which can also be wrapped into a zero-dimensional material called fullerene. Carbon atoms are arranged in a honeycomb lattice on a 2-D plane to form graphene. $sp^2$ orbitals are created through the hybridization of three carbon atomic orbitals. Covalent bonds are created between these $sp^2$ orbitals and the carbon atoms. The hybridised $sp^2$ orbitals and the 1.42 separation between the carbon atoms create the hexagonal planar structure known as the honeycomb lattice. Graphene's crystal structure gives rise to certain outstanding properties.[7] In the past several years, the arena of nanoscience and nanotechnology has emerged significantly and its application is increasing continually in different industries.[8] The interest in nanoscience has grown in academia and business since the creation of monolayer graphene. Researchers from all over the world are now very interested in graphene, which has been dubbed a "wonder substance" because of its excellent mechanical and functional qualities and high potential for creating advanced gadgets. Materials made of graphene have a lot of potential for use in electromechanical devices.[9]

Scientists have been attracted to the study of graphene and its derivatives such as graphene oxide (GO), reduced graphene oxide (rGO) because of their good properties, including their large specific surface area, strong chemical stability, good electrical conductivity, and potential optical, mechanical, electrical, and structural properties.[10] As a result, the nanocomposite materials based on graphene have good conductivity for energy storage and conversion due to all of the above features.[11] The focus of this review will be on the creation and functionalization of graphene-based nanocomposites, which have great potential for usage in energy storage and energy conversion applications.[12-14] In this research work, we apply r-GO dispersion solution in photoelectrochemical solar cells to investigate solar energy conversion and storage.

## MATERIALS AND METHOD

This section describes the materials that are used for the synthetization of graphite powder to graphite oxide and reduced graphite oxide, preparation for other solutions. Table 1 shows the chemicals and their specifications used for solutions.

**Table 1: Materials Used**

| S. No | Chemical | Specifications |
|---|---|---|
| 1 | Graphite power | Merck |
| 2 | EDTA di sodium salt | Loba chemical |
| 3 | Sodium hydroxide | Loba chemical |
| 4 | Oxalic acid | Loba chemical |
| 5 | Phenolphthalein | Loba chemical |
| 6 | 98%, Con.$H_2SO_4$ | Merck |
| 7 | >99%, $KMnO_4$ | Merck |
| 8 | De-ionized water | Loba chemical |
| 9 | 6%, $H_2O_2$ aqueous | Loba chemical |
| 10 | Diluted $HNO_3$ | Merck |
| 11 | Hydrazine hydrate | Merck |
| 12 | Acetone | Loba chemical |
| 13 | Methanol | Loba chemical |
| 14 | Ethanol | Loba chemical |
| 15 | 1-propanol | Loba chemical |

### Methods

### Synthesis of Graphite to Graphite oxide (GO)

In today's era, it is extremely difficult to manufacture graphene on a large scale. GO can be produced by oxidizing graphite, using a variety of techniques, including those shown by Brody, Staudenmaier's and Hummer. For the preparation of GO, the Modified Hummers method has been employed most frequently.[15]

In a typical experiment, 20 g of graphite powder (Merck) is mixed with $NaNO_3$ (10 g) to form a homogeneous solution. Now after this take 450 mL of concentrated $H_2SO_4$ (96% w/w) in a beaker of 5 L capacity. Now, an ice bath is used to cool the solution and keep the temperature below 5°C. Under steady stirring with a stirrer coated in Teflon, the two ingredients above were progressively combined. Additionally, while keeping the reaction mixture's temperature to below 5°C, gradually, 60 g of $KMnO_4$ (Merck) were added. The reaction mixture was removed from the ice bath after the $KMnO_4$ addition was finished and kept constantly stirring. The reaction mixture then appeared to transform into a brownish-gray paste. The reaction vessel's temperature was raised to 95°C by slowly adding 1000 mL of de-ionized water. Further dilution of the reaction mixture was accomplished using de-ionized water. The un-reacted $MnO_4$- and by-product $MnO_2$ were then converted into soluble $Mn^{2+}$ by reacting it with 6% $H_2O_2$. The resulting brown solution was dried at 50°C in a vacuum oven after being vacuum filtered and rinsed with diluted $HNO_3$ to eliminate any remaining metal ions from the graphite oxide.[16]

Graphene oxide (GO) must be reduced in order to regain its thermal and electrical properties because it's thermally unstable and electrically insulating. Graphite oxide is exfoliated and reduced to reduced graphene oxide predominantly through chemical processes Figure 1.

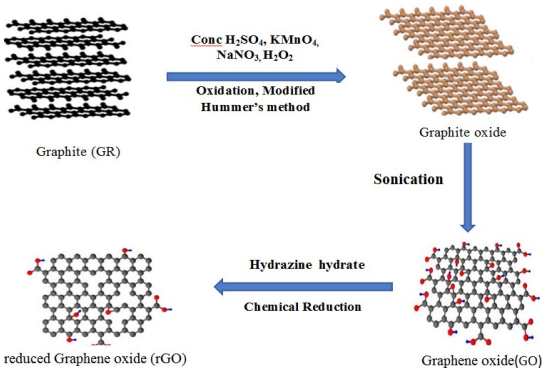


**Fig. 1. Schematic diagram formation from Graphite to Graphite oxide, Graphene oxide (GO) to reduced Graphene oxide (rGO)**

## Synthesis of Graphene oxide (GO) to reduced Graphene oxide (rGO)

To produce chemically reduced graphene oxide (rGO), graphite oxide was first converted into a stable colloidal dispersion and then employing reducing chemicals to reduce the exfoliated graphite oxide. Exfoliating graphite oxide with ultrasonication in either water or alcohol can result in the formation of a stable GO dispersion. r-GO was created by reducing agents reacting with graphene oxide. For this investigation, r-GO was obtained using hydrazine hydrate. The above suspension was once more sonicated for 2 h to produce rGO. At room temperature, hydrazine hydrate was gradually added drop by drop to the exfoliated graphite oxide suspension. The reduction took place for 1 h at 100°C For this sample, hydrazine hydrate and GO were maintained at a weight ratio of 9:7. The resulting black precipitates were then rinsed with a 1M HCl solution and filtered through cellulose filter paper. To extract rGO, the filtrate was dried for 24 h at room temperature.[17-19]

## Preparation of Solutions

All solutions are created with double-distilled water. The creation of all chemical stock solutions involves direct weighing. We employed several solutions, including. rGO dispersion solution, 1N NaOH solution, and .01M EDTA. The dry product was first crushed with a mortar and pestle to prepare rGO dispersions in various solvents. After that, the solvent was mixed, and the mixture were sonicated for an hour in an ultrasound bath cleaner.[20] To obtain a nominal concentration of 0.5 mg $mL^{-1}$ for all of the solvents, a specified quantity of rGO power (5 mg) was added to a predetermined volume of solvent (10 mL), allowing direct comparison between the dispersion behaviours of the various solvents. Acetone, methanol, ethanol, and 1-propanol were the organic solvents used to test rGO dispersions.[21] We have shown that the solubility of rGO varies depending on the solvent, being 0.9, 0.52, 0.91, and 1.2 correspondingly.[22] Compared to other organic solvents, 1-propanol has superior solvent solubility. The rGO and 1-propanol dispersions solution remained stable for several days without noticeable sedimentation.

## Experimental Section of the photoelectro chemical cell

The apparatus of the Photoelectrochemical cell having a dark H-shape glass tube with a transparent window for illumination.[23-25] In the H-shaped tube, the solution of graphene dispersed, NaOH and Reductant (EDTA) was filled in the proper manner. The total volume of the above tube after filling the solution was always 30 mL. After that in the H-shape glass tube which has a transparent window for the illumination, a platinum electrode was dipped with the saturated calomel (SCE) electrode combination. A digital multimeter was connected to the terminals of the electrodes. The apparatus measured the dark potential inside the chamber of total darkness. A lamp (tungsten) serving as the light source was exposed through the clear window of the apparatus. To filter infrared radiation, the light source and the illuminated chamber were separated by a water filter. The final step of the experiment was measuring the potential and current produced by the experimental setup using a digital multimeter. The current-voltage (i-V) characteristic of photoelectrochemical cells has been investigated by providing an external load with the support of a carbon pot (log 407 K) that was linked in the circuit through with a key to produce open circuit and close circuit device.[26-29]

## Mechanism of Current Generation

An electricity generator powered by (cyclic) light is the photoelectrochemical system. For numerous cycles, it has been observed that the

photoelectrochemical behaviour is reversible.[30] In the cell, the reducing agents and their oxidised residues provide as the electron carriers. Fig. 2. illustrates how the electron exchange between the electrode, photosensitizer (rGO), and reductant (EDTA) produces the photo current in a photoelectrochemical cell.[31-33]

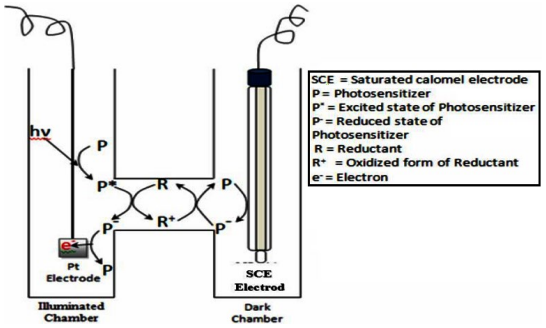


**Fig. 2. Scheme of mechanism of current generation**

These observations lead to the following mechanism is described for the production of photocurrent in the photoelectrochemical cell's:

$$rGO \longrightarrow rGO^* \quad (1)$$

$$rGO^* + R \longrightarrow rGO^- \text{ (Semi or leuco)} + R \quad (2)$$

$$rGO^- \longrightarrow rGO + e^- \quad (3)$$

$$rGO + e^- \longrightarrow rGO^- \text{ (Semi or leuco)} \quad (4)$$

$$rGO^- + R^+ \longrightarrow rGO + R \quad (5)$$

Where: rGO = reduced graphene oxide, rGO*=Excited reduced graphene oxide, $rGO^-$ =Semi form of reduced graphene oxide, R=reductant molecule, R+=Oxidized form of the reductant.

## RESULT AND DISCUSSION

### Study of photo potential with time during the charging of the cell

The changes in potential of the system with time were measured at different time intervals by digital multimeter. During the charging of a photoelectrochemical cell, the photopotential is gradually increased until it reaches its maximum value, after which it remains relatively constant, which is known as maximum photo potential ($V_{OC}$) and the curve is maximum increase and it remains relatively constant then decrease open circuit potential ($V_{OC}$).

A substance becomes more electrically conductive when electromagnetic radiation, such as visible light, infrared light, and UV light, is absorbed. A phenomenon of both optics and electricity is photoconductivity. When light is absorbed, more free electrons and holes become available, increasing the electrical conductivity of a graphene material. The term "photocurrent" refers to the flow of electricity caused by photoconductivity or the photovoltaic effect. Here, photoconductivity is the generation, migration, and recombination of free carriers in the conduction and valence bands is used to describe the photovoltaic process. Graphene's strong charge carrier mobility, wide range of light absorption, and ultrafast carrier dynamics make it a potential material for the production of high-performance photoelectrons.

The variation of photopotential of dispersed solution of rGO with EDTA system with respect to time is graphically represented in Figure 3.

**Table 2: Variation of Potential with Time**

| S. No | Time (min) | Photopotential (mV) | S. No | Time (min) | Photopotential (mV) |
|---|---|---|---|---|---|
| 1 | 0 | 463 | 9 | 80 | 838 |
| 2 | 10 | 481 | 10 | 90 | 1118 |
| 3 | 20 | 501 | 11 | 100 | 1134 |
| 4 | 30 | 539 | 12 | 110 | 1139 |
| 5 | 40 | 627 | 13 | 120 | 1140 |
| 6 | 50 | 667 | 14 | 140 | 1142 |
| 7 | 60 | 676 | 15 | 160 | 1141 |
| 8 | 70 | 680 | 16 | 180 | 1138 |

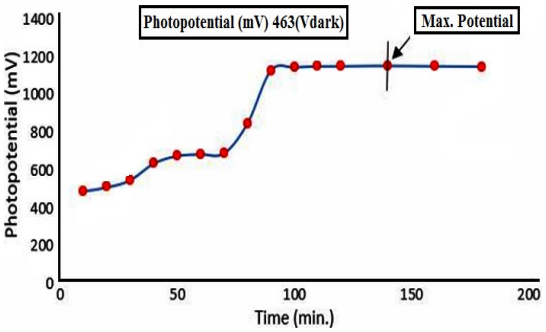


**Fig. 3. Variation of Potential with Time**

### Current–voltage (i-V) characteristics of cell

A digital multimeter (with one circuit closed) and a digital multimeter are used to measure the short circuit current ($i_{sc}$) and open circuit voltage ($V_{OC}$) in PECs (photoelectrochemical cells) (with the other circuit open). Close circuit potential is present when a key is put into the

switch. The extreme value between the potential and current readings was recorded when a digital multimeter connected to the circuit via a carbon pot (log 470K) applied an external load. Current-potential (i-V) characteristics of the photoelectrochemical cells are graphically represented in (Fig. 4) using an EDTA and dispersion solution of reduced graphene.

**Table 3: Variations of Photopotential with Photocurrent**

| S. No | Photopotential (mV) | Photocurrent (µA) | S. No | Photopotential (mV) | Photocurrent (µA) |
|---|---|---|---|---|---|
| 1 | 32 | 960 | 25 | 423 | 480 |
| 2 | 38 | 940 | 26 | 453 | 460 |
| 3 | 45 | 920 | 27 | 554 | 420 |
| 4 | 58 | 900 | 28 | 572 | 400 |
| 5 | 60 | 880 | 29 | 578 | 380 |
| 6 | 77 | 860 | 30 | 621 | 360 |
| 7 | 86 | 840 | 31 | 646 | 340 |
| 8 | 94 | 820 | 32 | 652 | 320 |
| 9 | 107 | 800 | 33 | 686 | 300 |
| 10 | 119 | 780 | 34 | 704 | 280 |
| 11 | 143 | 760 | 35 | 749 | 260 |
| 12 | 155 | 740 | 36 | 777 | 240 |
| 13 | 163 | 720 | 37 | 807 | 220 |
| 14 | 177 | 700 | 38 | 831 | 200 |
| 15 | 182 | 680 | 39 | 868 | 180 |
| 16 | 196 | 660 | 40 | 898 | 160 |
| 17 | 227 | 640 | 41 | 925 | 140 |
| 18 | 255 | 620 | 42 | 957 | 120 |
| 19 | 260 | 600 | 43 | 973 | 100 |
| 20 | 293 | 580 | 44 | 1012 | 80 |
| 21 | 331 | 560 | 45 | 1035 | 60 |
| 22 | 356 | 540 | 46 | 1064 | 40 |
| 23 | 370 | 520 | 47 | 1090 | 20 |
| 24 | 421 | 500 | 48 | 1112 | 0 |

In this i-v curve, we observed a point that is referred to the maximum power at power point ($P_{PP}$) since it is where the result of maximum current and minimum potential is found. The following formula is used to obtain the fill-factor at power point when the potential reading is greatest and the current reading is zero.

$$\text{Fill factor } (\eta)=(V_{PP}\times i_{PP})/(V_{OC}\times i_{SC}) \quad (6)$$

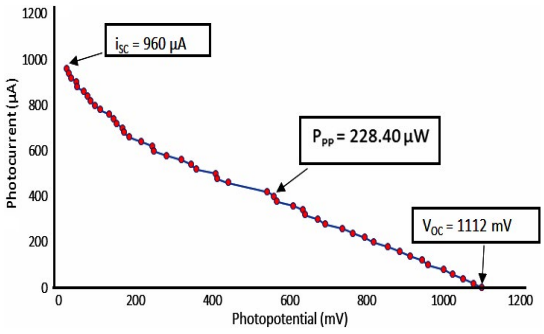


**Fig. 4. Photocurrent and Photopotential (i-V) Characteristics curve**

**Study of photopotential, photocurrent and power at power point of the cell**

Then key insert in connecting switch 20 µA difference in similar photocurrent in decrease and photo potential in continuously increase and photopotential and photocurrent are multiplied obtain power and after then we reach maximum power of the cell.

Graphical representations of the photo-potential, photocurrent, and power at power point of cell for photoelectrochemical cells with dispersed solution-EDTA system Figure 5.

**Storage capacity of the cell**

The system's storage capacity (performance) is measured when the illumination is turned off as soon as the potential reaches a constant value and after applying an external load (which needs current at the power point). The storage capacity is measured in the form of $t_{1/2}$, or the time it takes for the greatest power to decrease to half in complete darkness. The observed half-life of the cell is 1300 min, as shown graphically in Figure 6.

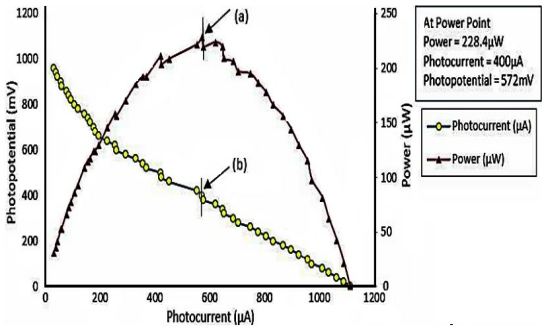


**Fig. 5. Variation of Potential and Power with Current (a) (i-V) Characteristic of the Cell, (b) Power v/s Current**

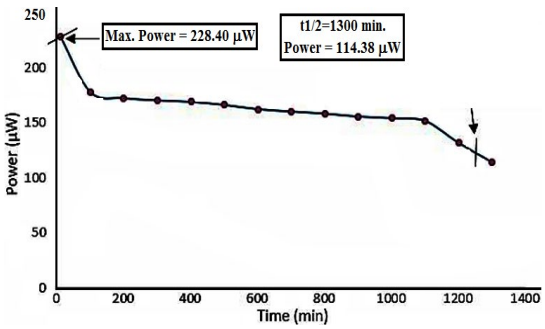


**Fig. 6. Study of cell performance**

**Table 4: Performance of the Cell**

| S. No | Time (min) | Power (μW) | S. No | Time (min) | Power (μW) |
|---|---|---|---|---|---|
| 1 | 0 | 228.4 | 24 | 690 | 160.38 |
| 2 | 30 | 200.78 | 25 | 720 | 160.05 |
| 3 | 60 | 184.72 | 26 | 750 | 159.23 |
| 4 | 90 | 177.99 | 27 | 780 | 158.42 |
| 5 | 120 | 176.46 | 28 | 810 | 157.61 |
| 6 | 150 | 174.93 | 29 | 840 | 157.12 |
| 7 | 180 | 173.06 | 30 | 870 | 155.82 |
| 8 | 210 | 172.21 | 31 | 900 | 155.85 |
| 9 | 240 | 171.87 | 32 | 930 | 155.5 |
| 10 | 270 | 171.02 | 33 | 960 | 155.18 |
| 11 | 300 | 170.52 | 34 | 990 | 154.37 |
| 12 | 330 | 170.18 | 35 | 1020 | 154.37 |
| 13 | 360 | 169.68 | 36 | 1050 | 154.06 |
| 14 | 390 | 169.17 | 37 | 1080 | 153.74 |
| 15 | 420 | 168.84 | 38 | 1110 | 151.74 |
| 16 | 450 | 167.16 | 39 | 1140 | 145.96 |
| 17 | 480 | 166.33 | 40 | 1170 | 139.41 |
| 18 | 510 | 166.33 | 41 | 1200 | 134.02 |
| 19 | 540 | 164.17 | 42 | 1230 | 128.97 |
| 20 | 570 | 163.84 | 43 | 1260 | 123.12 |
| 21 | 600 | 162.02 | 44 | 1290 | 117.13 |
| 22 | 630 | 162.02 | 45 | 1300 | 114.38 |
| 23 | 660 | 161.2 | 46 | 1320 | 112.66 |

## Conversion efficiency

The formula is used to determine the system's conversion efficiency, which is calculated to be 4.38% using the photocurrent and photopotential values at the power point and the incident power of radiations.

$$\text{Conversion efficiency}=(V_{PP}\times i_{PP})/(P\times A)\times 100\% \quad (7)$$

$$\text{Photo potential } (\Delta V)=V_{OC}-V_{Dark} \quad (8)$$

Here, open circuit voltage, potential at power point, short circuit current, current at power point, power of incoming light, electrode area, and dark potential are referred to $V_{oc}$, $V_{PP}$, $i_{sc}$, $i_{PP}$, P, A, dark $V_{Dark}$ as, respectively.

## Variation effect of photosensitizer (r-GO dispersed solution) on Photoelectrochemical cell

The effect of r-GO dispersed solution on photopotential and photocurrent was investigated. When the concentration of r-GO dispersion solution is increased, the photopotential, photocurrentand power of cellto their maximum value at 2 mL solution of rGO, after the obtain parameter are maximum and then decrease at given point in the studies of rGO and dispersion solution.

After varying the r-GO dispersed solution, it was observed that the lowest value shown in Table 5 for 1 mL r-GO dispersed solution, which has the lowest photopotential and photocurrent values at 432 mV and 642 μA, respectively. In a similar manner, the photopotential and photocurrent values at 2 mL are 1136 mV and 960 μA, respectively, while the power value is 1090.56 μW the highest in the graph.

In Fig. 7 show graphical representations of photo potential, photocurrent, and power of the cell with graphene distributed solution.

**Table 5: Variation of Potential, Current and Power with r-GO Dispersed solution**

| S. No | r-GO dispersed solution (mL) | Photopotential (mV) | Current (μA) | Power (μW) |
|---|---|---|---|---|
| 1 | 1 | 432 | 642 | 277.34 |
| 2 | 2 | 1136 | 960 | 1090.56 |
| 3 | 3 | 448 | 702 | 314.49 |
| 4 | 4 | 585 | 596 | 348.66 |
| 5 | 5 | 432 | 826 | 356.83 |

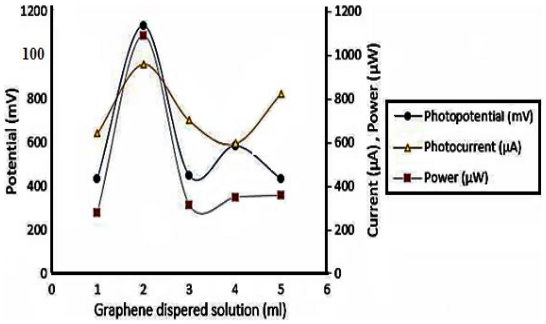


**Fig. 7. Variation of Potential, Current and Power with r-GO Dispersed solution**

### Performance of the Cell

The photoelectrochemical cell's total performance has been measured, and it has attained an impressive stage in terms of storage capacity, electrical output, conversion efficiency, and initial photocurrent generation.

**Table 6: All parameters are observed result in performance of the cell**

| S. No | Parameters | Observed Value |
|---|---|---|
| 1 | $V_{dark}$ (Dark potential) | 463mV |
| 2 | $V_{oc}$ (Open circuit Potential) | 1142mV |
| 3 | $V_{PP}$(Potential at power point) | 572mV |
| 4 | $i_{SC}$(Short circuit current) | 960μA |
| 5 | $i_{PP}$(Current at power point) | 400μA |
| 6 | Power of incident light | 10.4mW/cm$^2$ |
| 7 | Area of electrode | 0.5 cm$^2$ |
| 8 | $t_{1/2}$(Storage capacity) | 1300 min |
| 9 | (Conversion efficiency η) | 4.38% |
| 10 | Fill factor | 0.17 |
| 11 | Maximum power | 228.40μW |
| 12 | ΔV(Photopotential) | 679mV |

## CONCLUSION

Fossil fuels industries account for a sizable share of global electricity production. Although the observed conversion efficiency of PG cells is fairly low (4.38%) as compare to the theoretical conversion efficiency of these cells is about 24–35%. Periodically, there are discussions on this challenge to photogalvanic cell development. To hasten the implementation of climate change measures, the world will need to dramatically reduce its usage of coal and oil over the coming decades. At the moment, hydrocarbon materials provide about more than half of the world's energy needs. r-GO dispersed solution, NaOH, and EDTA are novel system for solar cell is more effective. The r-GO dispersed solution has increased the storage capacity and conversion efficiency of Photoelectrochemical cell that happens as a result of the photo galvanic action on the working electrode.

The conversion efficiency, $t_{1/2}$, and fill factor for the r-GO dispersed solution, NaOH, and EDTA novel systems are recorded as 4.38%, 1300 min and 0.17, respectively. Power point applications for the r-GO dispersed solution, NaOH, and EDTA system are current at short circuit, potential at open circuit, and power point of cell (pp) were also tested, and the results are as follows: 960 mV, 1142 mV, 228.40 μW.

## ACKNOWLEDGEMENT

The authors are thank full to Head of the Department of Chemistry at Jai Narian Vyas University in Jodhpur, Rajasthan (342005) for providing essential laboratory resources for carrying out this research.

### Conflict of interest

The author declare that we have no conflict of interest.

## REFERENCES

1. Malviya, A.; Solanki, P. P., *Renewable and Sustainable Energy Reviews.*, **2016**, *59*, 662-691.
2. Tale, B.; Nemade, K. R.; Tekade, P. V., *Polymer-Plastics Technology and Materials.*, **2021**, *60*(7), 784-797.
3. Mahmood, N.; Zhang, C.; Yin, H.; Hou, Y., *J. Mater. Chem. A.*, **2014**, *2*(1), 15-32.
4. Chori, H. J.; Jung, S. M.; Seo, J. M.; Chang, D. W.; Dai, L.; Beak, J. B., *Nano Energy.*, **2012**, *1*(4), 534–551.
5. Novoselov, K. S.; Geim, A. K.; Morozov, S. V.; Jiang, D.; Zhang, Y.; Dubonos, S. V.; Grigorieva, I. V.; Firsov, A.A., *Science.*, **2004**, *306*, 666-669.
6. Bich, N. H.; Van, N. H., *Advances in Natural Sciences: Nanoscience and Nanotechnology.*, **2016**, *7*, 1-16.
7. Madhad, H. V.; Vasava, D.V., *Journal of Thermoplastic Composite materials.*, **2019**, *35*(9), 1-29.
8. Wan, X.; Huang, Y.; Chen, Y., *Acc Chem Res.*, **2012**, *45*, 598–607.

9. Fu, X.; Yao, C.; Yang, G., *RSC Advances*., **2015**, *5*, 61688–61702.
10. Fernanda, T. M.; Vania, G. A.; Katia, N.; Marina, L. S.; Anderson, S.K., *Nanomedicine*., **2015**, 1-28.
11. Kim, K. K.; Reina, A.; Shi, V.; Park, H.; Lee, Y. H., *Nano technology*., **2010**, *21*, 285205.
12. Marian, M.; Vijay, T.; Florin, M.; Stefan, V., *Polymer advanced technologies*., **2016**, *27*, 844-59.
13. Ambrosi, A.; Pumera, M., *Chem. Eur. J*., **2016**, *22*, 153-9.
14. Lawal, A. T., *Biosensors and Bioelectronics*., **2019**, *141*, 111384.
15. Sharma, N.; Sharma, V.; Jain, Y.; Kumari, M.; Gupta, R.; Sharma, S. K.; Sachdev, K., *Macromol. Symp*., **2017**, *376*, 1700006.
16. Shams, S. S.; Zhang, R.; Zhu, J., *Materials Science-Poland*., **2015**, *33*(3), 566-578.
17. Cao, N.; Zhang, Y., *J. Nanomaterials*., **2015**, *2015*, 168125.
18. Tripathi, S. N.; Rao, G. S. S.; Mathur, A. B.; Jasra, R., *RSC Adv*., **2017**, *7*(38), 23615–23632.
19. Park, S.; Potts, J. J. R.; Velamakanni, A.; Murali, S.; Ruoff, R. S., *Carbon*., **2011**, *49*, 3019 -3023.
20. Zhang, X.; Coleman, A. C.; Katsonis, N.; Browne, W. R.; Wees, B. J. V.; Feringa, B. L., *Chemical Communications*., **2010**, *46*(40), 7539-7541.
21. Pardes, J. I.; Villar-Rodil, S.; Martı´nez-Alonso, A.; Tasco´n, J. M. D., *J. American Chemical Society*., **2008**, *24*, 10560-10564.
22. Johnson, D. W.; Dobson, B. P.; Coleman, K. S., *Current Opinion in Colloid & Interface Science*., **2015**, *20*(5-6), 367–382.
23. Gangotri,K.M; Meena, R.C., *J. Photochem. Photobiol.A: Chemistry*., **2001**, *141*, 175-177.
24. Ganwa, K. R.; Singh, S. S.; Singh, K., *J. Ind. Chem. Soc*., **2017**, *94*, 527-533.
25. Meena, P. K.; Meena, R. C.; Meena, S. L.; Meena, K., *Int. J. for Res. in Applied Sci. & Eng. Tech. (IJRASET).,* **2018**, *6*, 1472-1478.
26. Meena, R. C.; Meena, K., *Energy Sources Part A*., **2009**, *31*, 1081-1088.
27. Genwa, K. R.; Singh, A. P., *Asian Journal of Chemistry*., **2017**, *29*(6), 1215-1219.
28. Chandra, M., Meena, R. C., *J. Chem. And Pharm. Research*., **2011**, *3*(3), 264-270.
29. Meena, R.C.; Meena, S. L.; Saini, S. R., *Adv. in Chem. Eng. And Sci*., **2017**, *7*, 125-136.
30. Amogne, N. Y.; Ayele, D. W.; Tsigie, Y. A., *Materials for Renewable and Sustainable Energy.,* **2020**, *9*(4), 1-6.
31. Koli, P., *Arabian Journal of Chemistry*., **2017**, *10*(8), 1077-83.
32. Jurasz, J.; Canales, F. A.; Kies, A.; Guezgouz, M.; Beluco, A.; *Solar Energy*., **2020**, *19*, 703-24.
33. Meena, S.L.; Meena, P.K., *J Adv Sci. Res*., **2021**, *12*(2), 110-116.